Buckling properties of 2D regular elastomeric honeycombs

1997 J. Phys.: Condens. Matter 9 L323

(http://iopscience.iop.org/0953-8984/9/22/002)

J. Phys.: Condens. Matter **9** (1997) L323–L329. Printed in the UK PII: S0953-8984(97)82700-2

LETTER TO THE EDITOR

Buckling properties of 2D regular elastomeric honeycombs

S Hutzler and D Weaire
Physics Department, Trinity College, Dublin, Ireland

Received 17 March 1997

Abstract. The buckling properties of a 2D regular honeycomb are studied using a model in which each edge is subject to local elastic forces associated with stretching and bending. A discretized version of the model is used to simulate the buckling of honeycombs under various combinations of axial strains. No complex buckling patterns with large unit cells have yet been found. This is contrary to some experimental results, which are attributed to wall effects. In other respects our results roughly confirm and extend previous estimates of the buckling transition.

The buckling of a regular honeycomb has been invoked as an elementary prototype for the progressive collapse under stress of solid foams [1]. In addition, such honeycombs have some direct interest since they are fabricated for structural uses [1]. From the theoretical point of view the buckling of such a lattice structure provides interesting examples of symmetry breaking.

In this Letter we introduce a simple model for the elastomeric honeycomb and explore its properties. No plastic or brittle properties are attributed to the constituent material, in contrast to some recent work by Silva and Gibson [2, 3]. Instead we concentrate on the simplest case and allow some generality in the type of strains imposed and the key parameters of the model. We have made a larger number of computations in this spirit from which there emerges an appealing, if not yet fully developed, picture of the buckling behaviour of the system.

The unstrained honeycomb (figure 1) consists of straight edges. Here we will take the term *buckling* to refer to any curvature of these sides, developed under strain. With such a definition, buckling occurs immediately upon imposition of *any* strain other than isotropic extension/compression. However if the strain is a combination of extension/compression along the two axis x and y indicated in figure 1, then in general only partial buckling occurs at low strain. Some edges remain straight on account of symmetry and are buckled only at a certain critical value of strain (or stress). This transition has been the point of primary interest in previous work [1] (and references cited therein), as it is here. Most references to buckling in what follows refer to this transition. We will identify the critical point under various combinations of x and y strains. Among these the most important in practice is the case which corresponds to uniaxial stress, in which the stress in the x or y direction is maintained at a finite value while the other dimension is unconstrained.

The model used is related to the theory of thin beams and may be found for example in the book by Landau and Lifshitz [4]. The energy of the honeycomb is written as a sum of local stretching and bending contributions:

$$E = E_{stretch} + E_{bend}. \tag{1}$$

The stretching energy is given by

$$E_{stretch} = \frac{1}{2}k_s \int \left(\frac{\mathrm{d}l}{\mathrm{d}l_0} - 1 \right)^2 \mathrm{d}l_0. \tag{2}$$

Here each point in the beam is a distance l from one end, where l_0 is the value for zero strain. The important parameter k_s determines the elastic resistance to stretching.

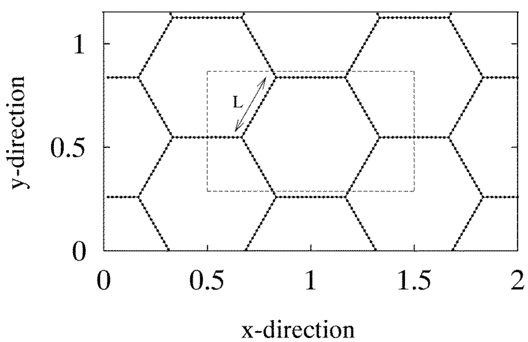

Figure 1. The undeformed honeycomb structure. The axes used for imposed strains and discrete points used for a typical computation are indicated. Most calculations were performed with the unit cell shown by a dashed line, and L = 1/3 in all cases.

Similarly the bending energy may be written

$$E_{bend} = \frac{1}{2}k_b \int c^2 \mathrm{d}l_0. \tag{3}$$

where c is the local curvature, and the parameter k_b determines the elastic resistance to bending. The angles at vertices remain fixed at 120^o.

In thin beam theory these two parameters are given by

$$k_s = Yd \tag{4}$$

$$k_b = Y\frac{d^3}{12} \tag{5}$$

where Y is the Young's modulus of the two-dimensional beams of length l and width d which corresponds to the edges. Alternatively, in the case of a real honeycomb, it is the Young's modulus of the constituent material multiplied by its thickness in the third dimension. No account is taken here or elsewhere of the finite size of the junctions, represented as vertices.

It follows that, to lowest order, the above energy describes an elastomeric honeycomb made up of beams of such width that they occupy a fraction ϕ of its area, according to

$$\phi = \frac{2}{\sqrt{3}}\frac{d}{L}. \tag{6}$$

For many purposes, the most significant parameter of the model is the dimensionless ratio k_b/L^2k_s. In all of the calculations presented here, $L = \frac{1}{3}$. Thus setting $k_b/L^2k_s = 9 \times 10^{-4}$ for example gives $\phi = 0.12$.

In order to reduce the problem to one of a finite number of variables, as necessary for computation, we take two steps. Firstly the continuous curves which constitute the edges (or thin beams) are represented by discrete points, typically about fifteen points per edge, as in figure 1. This is an elementary procedure which is detailed elsewhere; it requires special care only at the vertices. Secondly we impose periodicity on the deformed system with some unit cell which contains an integer number of honeycomb cells. For many purposes the number could be one, but in general we used two (as shown in figure 1) and in some cases more than two. It is important in any analysis of buckling which proceeds in such a manner to remember that the real system has no such periodic constraint, so that the provisional results obtained must be interpreted with caution.

The implementation of the model in a computer code, using the conjugate gradient method to minimize energy under imposed strain, was tested thoroughly by calculation of linear elastic properties. For example, the shear modulus G^*, computed using extensional shear, is shown in figure 2 as a function of k_b/k_s. There is only a small systematic discrepancy between the computed results and the exact analytic one [5], which is

$$G^*/k_s = \frac{k_b/k_s}{\sqrt{3}L\left(\frac{L^2}{12}+\frac{k_b}{k_s}\right)}. \tag{7}$$

Note, in particular, the linear dependence of G^* on k_b at low k_b/k_s. This is the regime of main interest, since real foams and honeycombs usually have ϕ of the order 0.1 or less (see equation (6)). Indeed, Gibson and Ashby implicitly take k_s to be infinite at the very outset. However, both conceptually and computationally, we have found it advantageous to maintain a finite (but usually large) value of k_s/k_b in this model.

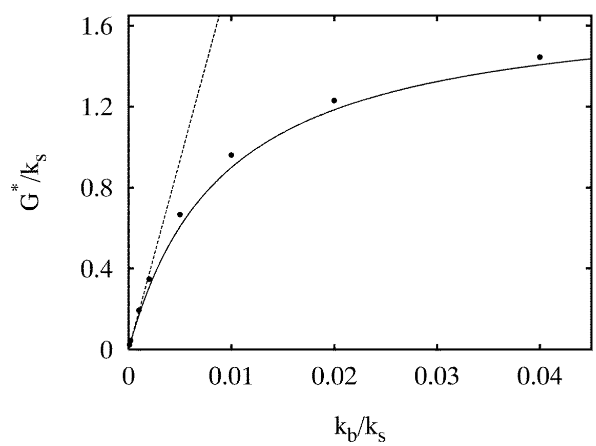

Figure 2. Shear modulus as a function of k_b/k_s, the ratio of bending and stretching force constants. The full line is the exact result [5] and computed values are shown as points. The dashed line corresponds to $k_s = \infty$ [1].

We have calculated the deformation of the honeycomb and the associated change in elastic energy, for various cases involving biaxial strains (ϵ_x, ϵ_y), whose positive values correspond to extension along the x and y axes of figure 1. Examples are shown in figures 3 and 4 and figure 5 shows the locus of the buckling transition in the (ϵ_x, ϵ_y) plane. Its location is usually obvious from graphical output but note that in some cases, such as that in figure 3(b), there can be an overshoot, i.e. a culmination of the unbuckled state. This is a numerical artefact.

For small compressive strains, these results take a simple form which may be rationalized as follows if we associate a critical force with buckling of a single beam [1].

To lowest order in k_b/k_s the stress resulting from an imposed biaxial strain (ϵ_x, ϵ_y) is isotropic, since we ignore the shear modulus to this order. This stress is proportional to

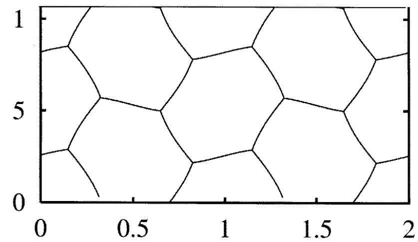

(a)

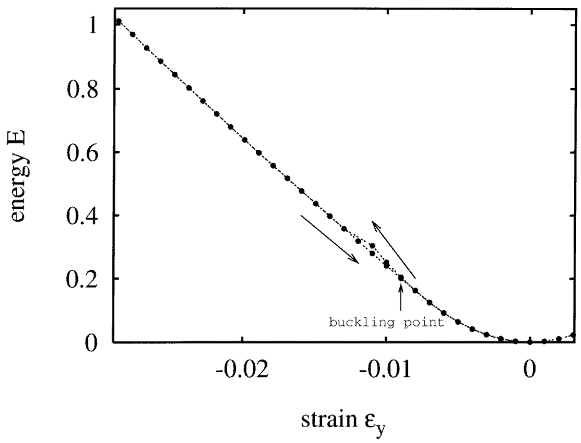

(b)

Figure 3. (a) Structure resulting from buckling transition under uniaxial strain, imposed as compression in the y direction ($\epsilon_y = 0.03$), for $k_b/L^2k_s = 9 \times 10^{-4}$. (b) The dependence of energy upon strain ϵ_y for uniaxial strain, calculated with the unit cell of figure 1. We show energy E of this unit cell as obtained from a strain cycle, where the structure is first strained beyond the buckling point and then brought back to a slight extension in the y direction ($\epsilon_y > 0$).

$k_s(\epsilon_x + \epsilon_y)$ and hence the critical strain for buckling is given by

$$k_s(\epsilon_x + \epsilon_y) = constant. \tag{8}$$

This line, of slope unity, is roughly consistent with figure 5, for small strains in the (-,-) quadrant.

The case of $\epsilon_x = \epsilon_y$ (uniform compressive strain) is interesting, in that it buckles in the same uniaxial manner as does the case of $(0, \epsilon_y)$. However, the important case of uniaxial stress (the condition for which Young's modulus is defined in linear elasticity) requires a much more subtle analysis. These calculations were performed by imposing a strain in one direction and relaxing the other dimension of the cell to minimize energy. It is clear from the results that the nonlinear corrections to equation (8) and the Poisson ratio are both important. Note in particular that the Poisson ratio rapidly departs from the value of linear elasticity as strain is increased.

We find a critical strain $\epsilon_x \simeq -0.08$ for compression on the x axis and no buckling transition in the other direction. These results are in rough agreement with the estimate and experiments of Gibson and Ashby [1].

The lack of any buckling for compression in the y direction under the condition of

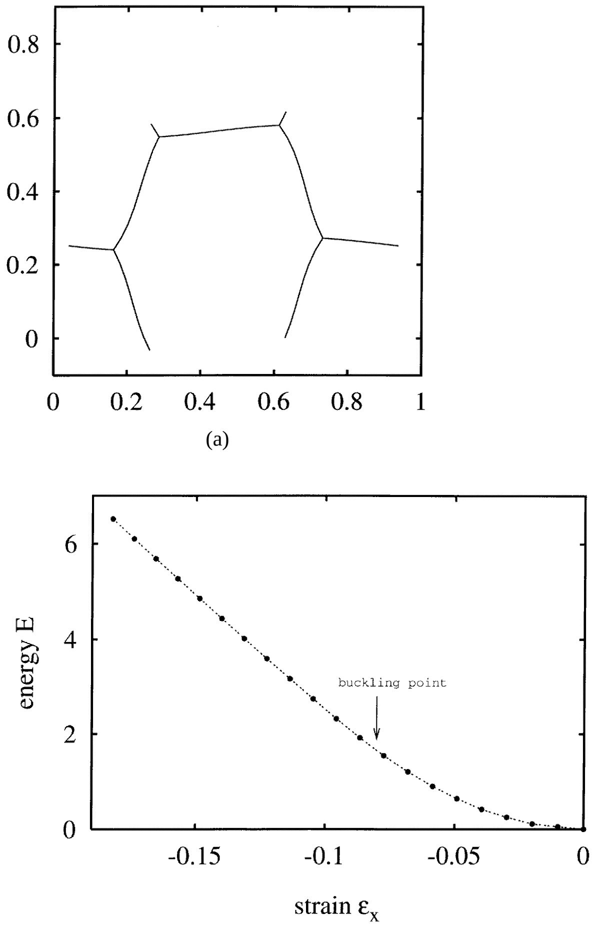

(b)

Figure 4. (a) Unit cell resulting from buckling transition under uniaxial stress, imposed as compression in the x direction ($\epsilon_x = 0.095$), for $k_b/L^2k_s = 9 \times 10^{-4}$. (b) The dependence of energy upon strain ϵ_x for uniaxial compressive stress in the x direction, calculated with the unit cell of figure 1. E is the energy of the unit cell. As in the case of uniaxial strain the energy curve exhibits no point of inflexion in the range shown, which would be indicative of localized collapse in a large system.

uniaxial stress (in the y direction) is an elementary consequence of the fact that the beams that are candidates for buckling are in the direction of zero stress. The locus of the buckling transition approaches close to, but never crosses, the line defined by Poisson's ratio in figure 5, for this case. This anisotropy in the behaviour of the honeycomb makes it difficult to relate its behaviour to that of a disordered network. This is similar to the situation in liquid foams in which topological changes depend strongly on orientation of stress [6].

We must now return to the caveat already noted; these are results based on a small periodic unit cell. Are they relevant to an infinite honeycomb without such constraint? In the important case of uniaxial stress we believe that the answer is yes. In neither case does there appear to be any indication of a point of inflection in curve of E against ϵ which would indicate *localized* buckling analogous to phase separation [1].

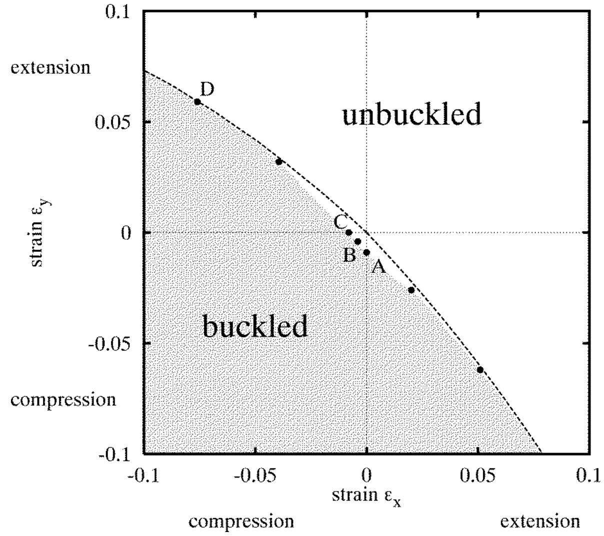

Figure 5. The locus of the buckling transition is shown as the edge of the shaded area. Calculated points include A,C (uniaxial strains), B (uniform compressive strain), D (uniaxial stress). The last point is located on the dashed line, which is defined by the numerically determined Poisson ratio for finite strains, under condition of compression in the x or y direction.

The case of uniaxial strain relates to an experiment of Gibson and Ashby [1]. The latter is described as a *biaxial stress* experiment, which it is, but examination of the deformed structure indicates it was obtained under uniaxial strain. Instead of the pattern which we would predict on the basis of our simulations (figure 3), a complex buckling pattern, with eight honeycomb cells in the periodic unit, was observed in the experiment as in [1] (p 99).

However, when an appropriate unit cell (consisting of eight honeycomb cells) was adopted for our calculation, this beautiful structure was not seen. Instead the more elementary buckling pattern (roughly similar to figure 3(a)) was again found. How can this serious discrepancy be resolved?

We believe the answer lies in the manner in which the experiment was performed. Not only was the sample small (which tends to suppress localized buckling) but it also appears to have been retained by *flat walls*, which are incompatible with the simple buckling pattern of figure 3(a). The occurrence of the complex pattern is likely to be a finite size and wall effect and not a property of the infinite system or larger samples.

Whether complex buckling patterns occur at all without hard walls or other constraints which favour them is a fascinating question to which the answer may well be 'no'.

Finally, we should note that many of our results conform well to an elementary theory in which different modes of deformation, with different dependencies on k_s and k_b, are in competition with each other.

Figure 3(b) is a good example. The initial buckling mode has an energy approximately proportional to $k_s\epsilon^2$. Eventually a lower energy buckled state exists because an alternative mode has energy approximately proportional to $k_b\epsilon$. These proportionalities emerge from the computation and may be rationalized by simple constraint-counting arguments. They are consistent, as is the previous argument given above, with the following rule for this type of buckling transition

$$\epsilon_{crit} \propto \frac{k_b}{k_s} \tag{9}$$

which was confirmed by computation for a wide range of k_b/k_s. It is not necessarily to be inferred that ϵ_{crit} goes to zero for $k_s \to \infty$, since higher-order corrections enter into that limit, and we believe that even at this small uniaxial strain is required for buckling.

Such a picture neglects the small amount of mixing of the two modes, and hence does not purport to describe the fine details of the transition.

The further development of this theory and its extension to the more difficult case of uniaxial stress will be undertaken in further studies. In addition, the predictions of the model for disordered foam networks will be determined, and plastic/brittle materials will be modelled. Already we would claim that this could well be regarded as the canonical elementary model for this problem, although there will always be ambiguity and choice in the definition of such an elastic model for finite strains.

SH is a TMR Fellow, contract ERBFBICT960970. This work was completed during a visit to the IST, Lisbon (DW: TMR Fellowship ERB4001GT957474), and supported by Forbairt and Shell, Amsterdam. We thank M Fortes, F Vaz, L Gibson, S Coughlan, F Bolton and R Phelan for advice and L Feria also for provision of computational facilities.

References

[1] Gibson L J and Ashby M F 1988 *Cellular solids: Structure and Properties* (Oxford: Pergamon
[2] Silva M J, Hayes W C and Gibson L J 1995 *Int. J. Mech. Sci.* **37** 1161
[3] Silva M J and Gibson L J 1997 *Int. J. Mech. Sci.* **39** 549
[4] Landau L D and Lifshitz E M 1986 *Theory of Elasticity* 3rd edn (Oxford: Pergamon)
[5] Dimitrovová Z 1996 *PhD thesis* IST, Lisbon
[6] Weaire D and Fortes M A 1994 *Adv. Phys.* **43** 685